Type: Original Research Paper / Tipo: Artículo Original de Investigación
Section: Optoelectronics / Sección: Optoelectronics

Measurements of the forward and backward scattering lobules, in six different Ar and He-Ne laser lines, passing through fog with different densities and fitted with the Henyey-Greenstein phase function

Medición de los lóbulos de dispersión frontal y posterior, en las líneas láseres de Ar y He-Ne, al atravesar neblina con diferentes densidades y ajustadas con la función de fase de Henyey-Greenstein

E. Reynoso Lara[1,*], G. Serrano Muñoz[1], J. A. Davila Pintle[1], M. Rendón Marín[1], M. D. Iturbe Castillo[2,A], C. G. Treviño Palacios[2,A]

1. Faculty of Sciences. of Electronics, Benemérita Universidad Autónoma de Puebla, Mexico.
2. National Institute of Astrophysics, Optics and Electronics (INAOE), Mexico.

(*) Email: ereynoso@ece.buap.mx A: miembro de AMO / AMO member

Received / Recibido: 17/08/2012. Revised / Revisado: 05/02/2014. Accepted / Aceptado: 20/02/2014.
DOI: http://dx.doi.org/10.7149/OPA.47.1.13

ABSTRACT:

In this work we show the results of, size distribution of water droplets measured in the lab, depolarization ratio, as well as extinction coefficient, of five lines from Ar laser and 632.8 nm of the He-Ne, when the beam laser pass through a fog chamber with different densities. The results obtained are in close agreement with those obtained in the literature. With the construction of a fog chamber, we could measure the angular width of the forward scattering lobule. We note that the best fit for the size distribution droplets was the generalized gamma function. Once obtained the value constants, of the gamma function, than better fitted the frequency histogram, we got the density number of droplets per volume unit. Although most studies have focused on the backscattering of light by different means, mostly clouds; however, the study of forward scattering lobule have been studied with great precision in many factors, such as the existence of single or multiple scattering and the amount that was performed.

Key words: Back and Forward Scatter, Depolarization Ratio, Broadening of the Beam.

RESUMEN:

Se presentan los resultados de las mediciones en laboratorio de la distribución del tamaño de gotas de agua, la razón de despolarización, el ancho angular del lóbulo de dispersión frontal; así como el coeficiente de extinción de cinco diferentes líneas de un laser de Argón y una a 632.8 nm de un laser de He-Ne, cuando el haz láser pasa a través de una cámara de neblina de gotas de agua con diferentes densidades. Los resultados obtenidos están en gran concordancia con los obtenidos en la literatura. Se observó que el mejor ajuste para la distribución del tamaño de las gotas, fue con la función gamma generalizada. Una vez que se obtuvieron el valor de las constantes, de la función gamma, que mejor ajustaron el histograma de frecuencia se obtuvo el número de densidad de gotas por unidad de volumen. Aunque la mayoría de los estudios realizados, se han centrado en la retrodispersión de la luz por diferentes medios, principalmente nubes; sin embargo, el estudio del lóbulo de dispersión frontal se han podido estudiar con extrema precisión muchos factores, tales como la existencia de simple o múltiple dispersión y la cantidad en que se llevó a cabo.

Palabras clave: Dispersión Retro y Frontal, Razón de Despolarización, Ensanchamiento del Haz.

REFERENCES AND LINKS / REFERENCIAS Y ENLACES

[1]. P. Bo, D. Tianhuai, W. Peng, "Propagation of polarized light through textile material", *Appl. Opt.* **51**, 6325-6334 (2012). DOI

[2]. B. Baumann, S. Baumann, T. Konegger, M. Pircher, E. Götzinger, F. Schlanitz, C. Schütze, H. Sattmann, M. Litschauer, U. Schmidt-Erfurth, C. K. Hitzenberger, "Polarization sensitive optical coherence tomography of melanin provides intrinsic contrast based on depolarization", *Biomed. Opt. Express* **3**, 1670-1683 (2012). DOI

[3]. E. E. Gorodnichev, S. V. Ivliev, A. I. Kuzovlev, D. B. Rogozkin, "Transmission of polarized light through turbid media", *Opt. Spectrosc.* **110**, 586-594 (2011). DOI

[4]. S. Prashant, P. Asima, "Polarization-gated imaging in tissue phantoms: Effect of size distribution", *Appl. Opt.* **48**, 6099-6104 (2009). DOI

[5]. R. Bradley, P. Arkady, "Hybrid modeling of electrical and optical behavior in the heart", *Physica D* **238**, 1019-1027 (2009). DOI

[6]. J. S. Ryan, A. I. Carswell, "Laser beam broadening and depolarization in dense fog", *J. Opt. Soc. Am.* **68**, 900-908. (1977). DOI

[7]. D. Deirmendjian, "Scattering and polarization properties of water clouds an hazes in the visible and infrared", *Appl. Opt.* **3**, 187-196. (1964). DOI

[8]. M. Nicolet, M. Schnaiter, O. Stetzer, "Circular depolarization ratios of single water droplets and finite ice circular cylinders: A modeling study", *Atmos. Chem. Phys.* **12**, 4207-4214 (2012). DOI

[9]. B. van Diedenhoven, A. M. Fridlind, A. S. Ackerman, "Influence of humidified aerosol on lidar depolarization measurements below ice-precipitating Arctic stratus", *J. Appl. Meteorol. Clim.* **50**, 2184-2192 (2011). DOI

[10] http://www.titantoolsupply.com/; Link principal de la empresa Titan tool Supply Co.

[11]. D. A. Skoog, J. J. Leary, *Análisis Instrumental*, 4th Edition, McGraw-Hill, pp. 142-148 (1992).

[12]. W. Demtröder, *Laser Spectroscopy: Basic Concepts and Instrumentation*, Springer-Verlag, pp. 42-44 (1982).

[13]. J. H. Scofield, "Frequency-domain description of a lock-in amplifier", *Am. J. Phys.* **62**, 129-133 (1994). DOI

[14]. D. Toublanc, "Henyey-Greenstein and Mie phase functions in Monte Carlo radiative transfer computations", *Appl. Opt.* **35**, 3270-3274 (1996). DOI

1. Introduction

Lidar techniques have been extensively applied to clouds observation and atmospheric aerosols monitoring, it has created the necessity of more precise information of the effects on the means of beam propagation. Most studies until now have mainly been concerned with measures of light backscattered, because is the available radiation in an atmospheric experiment. Light scattered in many materials have been matter of study [1-5], specially in water fog [6-9].

When the scatterers have spherical symmetry and are larger than the wavelength of incident light, like water droplets, a considerable fraction of the light is scattered in a narrow angular lobule in the forward direction. In some atmospheric clouds, for example, the forward and backward dispersion may exceed 1000 to 1 in visible wavelengths. For water droplets with a diameter slightly larger than the wavelength, diffraction theory can be used to estimate the angular half-width of the forward scattering lobe. That is; clouds in the atmosphere containing droplets of several microns in diameter; the width of the forward lobule is only a few degrees at visible wavelengths, but larger than the backward lobule. This is of great importance in the estimation of lidar returns from clouds of high optical depth, since the beam width of the forward lobule gives information on how much light is scattered in a given field of view. These lobules can be fitted through phase functions that depend of scattering angle, mainly.

The purpose of this work is verify the pattern of scattering of light for water droplets, following the steps that Ryan and Carswell made

in [6], but with different experimental setup; and to establish a method to characterization of different scatterers both liquids and solids. This will help to researchers to know the shape of the phase functions of each scatterer.

2. Methods and results

2.1. Size radius measurements of the water droplets

The diameter of the water droplets was measured from artificial fog, generated by ultrasonic humidifier, which is the scattering media. In order to do accurate measurements in a micro-scale, there was the necessity to obtain a physical reference frame, that is, a scale which it could be measure the diameter of water droplets.

As a scale reference, a measuring microscope Titan model TM-II [10] was used to measure the geometrical cells on a shell of garlic, getting a physical reference grid of 10 μm as a metric ruler. Each one droplets sample was placed in the microscope to take a picture. That picture was overlapped with the reference grid (10 μm), to do an accurate count of the droplets with different diameters. The procedure was repeated thoroughly with a large sample.

The result from the count is a histogram of the size distribution of water droplets, which is shown in Fig. 1. From that plot we see an asymmetric distribution, which fits fairly well the generalized gamma function of the type proposed by Deirmendjian [2], given by the following equation:

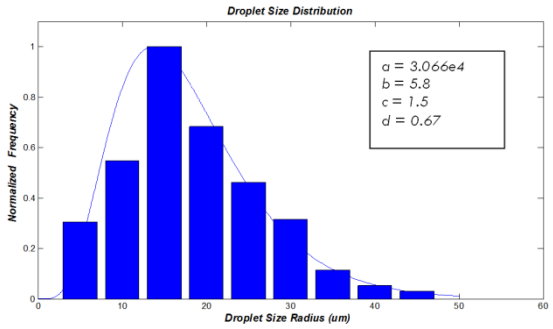

Fig. 1. Histogram of droplet size distribution fitted with a generalized gamma function.

$$n(r) = ar^b \exp(-cr^d), \qquad (1)$$

where $n(r)$ is the volume concentration, r is the radius and the positive constants a, b, c, and d are manipulated to obtain the best fit; the inset shows this values.

From Fig. 1, it is seen that the critical radius, where the concentration is maximum, is in 15 μm, unlike to the plot obtained by Ryan [1]. It is believed that the difference of the size droplets water is due mainly to different work frequencies from the nebulizer and humidifier used in those experiments, being those of 1.35 and 1.7 MHz, respectively.

Knowing the best values (inset, Fig. 1) from generalized gamma, the droplet number density is calculated through:

$$N = a \int_0^\infty r^b \exp(-cr^d) dr. \qquad (2)$$

Figure 2 shows the experimental setup for measuring the extinction coefficient through the

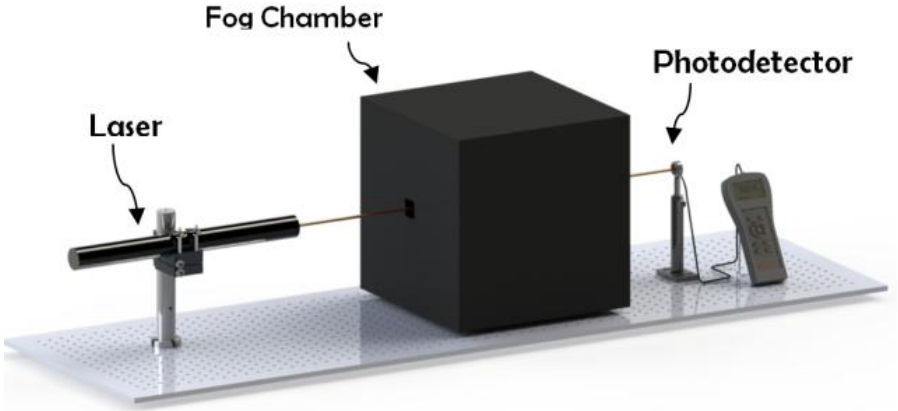

Fig. 2. Experimental setup to measure the extinction coefficient.

Beer-Lambert law [11,12]:

$$I_o = I_i \exp(-\alpha_{ext} z), \qquad (3)$$

where I_o and I_i are the output and input laser intensities to the fog chamber, respectively.

In order to maintain a constant average density fog, a chamber of one cubic meter from hard black poly-vinyl chloride (PVC) was built, with two windows in opposite sides, so that the beam light passed through the chamber. The extinction coefficient is given by:

$$\alpha_{ext} = \alpha_a + \alpha_s, \qquad (4)$$

where α_a and α_s are the attenuation and scattering coefficients, respectively.

The attenuation coefficient was considered equal to zero ($\alpha_a = 0$), because absorption is neglected. Therefore, the extinction coefficient is only the scattering coefficient. Thus, from Eq. (3):

$$\alpha_{ext} = -\frac{1}{z} \ln\left(\frac{p_o}{p_i}\right), \qquad (5)$$

where it was assumed that the areas from the laser beam is not divergent.

2.2 The extinction coefficient measurement in the lab for different wavelengths and fog densities

In order to average the extinction coefficient, several measurements were performed to assure a precise estimation by varying: the wavelength and the incident power from the laser, as well as the density fog within the chamber.

The Argon laser lines used in the experiment were 457, 476, 488, 496 and 514 nm, with powers of 3, 5.5, 20, 14, and 16 mW respectively. Besides, the 632.8 nm line from a He-Ne laser was also used, with a power of 17.5 mW. For each wavelength four measurements were made with different incident powers. To change the power of the laser, transmittance filters for the visible region with optical densities (OD) of 1, 0.5 and 0.3 were used. That is, transmittances were of the 10, 30, 50 and 100%, this last without filter. The density fog in the chamber was modified with different amplitudes of the acoustic frequency from the ultrasonic humidifier which is responsible for generating the fog to study. The normalized averaged results to different wavelengths are plotted in the Fig. 3.

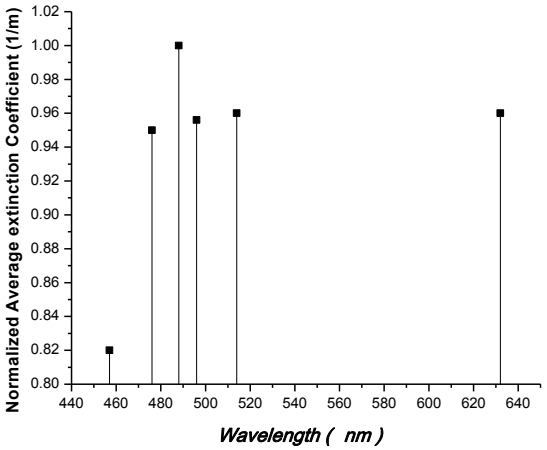

Fig. 3. Normalized extinction coefficient for different wavelengths.

It is evident from Fig. 3 that, at the wavelength of 457 nm, there is the biggest attenuation. That is because is closer to the window of maximum attenuation, besides of the lowest power. In this wavelength would be important to take $\alpha_a \neq 0$.

Finally, the average total extinction coefficient was calculated from the measurements done, giving $\alpha_{ext} = 3.71$ m^{-1}.

2.3 Depolarization in the fog

The depolarization effects are very important in the scattering process, since it is characteristic of the size, shape and refractive index, among others parameters, to each kind of scatterer. Laser sources are usually linearly polarized. The experimental setup to measure the light depolarization by fog is shown in Fig. 4.

The experimental setup consists in a linearly polarized laser source, two Glan-Thomson polarizers, the fog chamber, and a photodetector system (PDS), comprised for a photodetector head, a chopper and a lock-in amplifier [13]. The drive chopper frequency was 100 Hz. The first polarizer P_1, which was located immediately

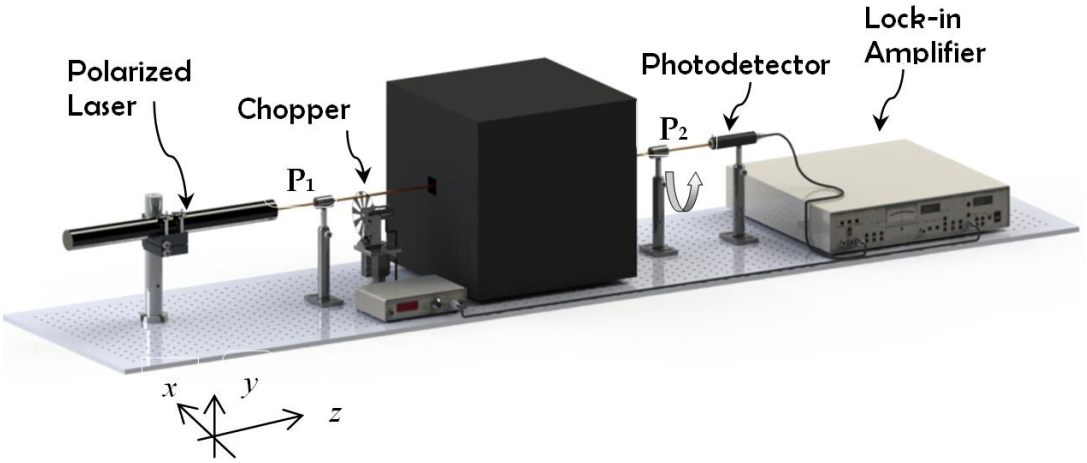

Fig. 4. Experimental setup to measure depolarization of water droplets. P_1 and P_2 are Glan-Thomson polarizers. P_2 is a rotating analyzer.

after source, enhances the polarization ratio 1000:1. P_2 is a polarization analyzer. P_2 mounted on a rotating stage in order to discriminate the two components of polarization, parallel and perpendicular to the input polarization.

In order to measure how the water droplets affect the polarization light when passes through the fog, the depolarization ratio is a convenient parameter to describe the state of polarization from a beam light, which is defined as

$$\delta = \frac{I_2}{I_1}, \qquad (6)$$

where I_1 is the output irradiance from the rotating polarizer, when its transmission axis is parallel to the polarization beam laser, and I_2 is the irradiance measured when the axis is perpendicular aligned (crossed polarizer) to the first polarizer. This irradiances are proportional to the electrical signal generated by the rotating polarizer which is periodical. Its maximum (V_{max}) occurs when the transmission axis of the polarizer is parallel to the oscillation plane of the input irradiance, and the minimum (V_{min}) when it is cross polarized. Therefore, when the polarization ratio (depolarization) changes, the amplitude also varies. This variation is detected by the lock-in amplifier as $\delta = \bar{V}_{max}/\bar{V}_{min}$, where the bars onto the voltages means average values.

Figure 5 shows the depolarization rate with respect to the transverse distance to propagation axis, to the wavelength of 632.8 nm.

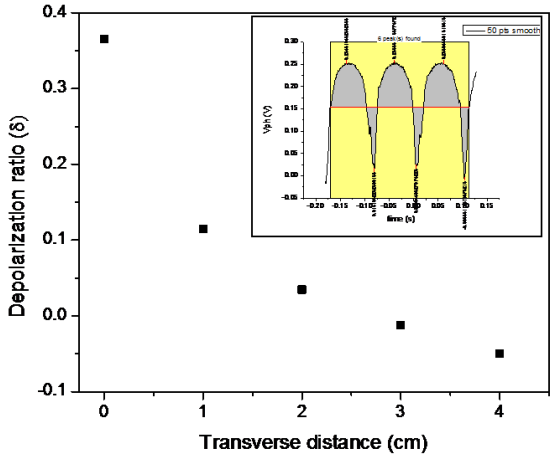

Fig. 5. Depolarization ratio of the beam light at 632.8 nm. In the inset, the electrical signal of the photoreceiver.

This data are obtained by signals like the inset of this figure. In this inset, we see the photodetector voltage (V_{ph}) proportional to the incident optical power; three cycles of V_{ph} are shown, where the maximums and minimums values belongs to the positions parallel and perpendicular of P_2 with respect to P_1, respectively.

The data measured with the experimental setup of Fig. 4 were measured at the output of the rotating polarizer in different perpendicular planes to the propagation axis, with transverse displacements to the beam laser. These were plotted in a polar coordinate system in Fig. 6. These data make a broad and large lobule in the

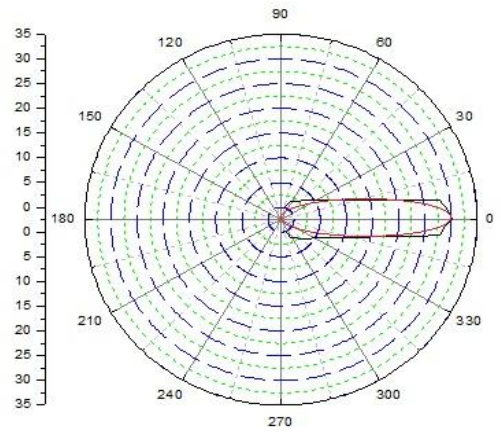

Fig. 6. Fitting of experimental results with the Henyey-Greenstein phase function.

forward scattering direction and small one in the backscattering. This plot was fitted with the Henyey-Greenstein phase function [14], by means of the next equation:

$$p(\theta) = \frac{1-g^2}{4\pi}\left(1+g^2-2g\cos(\theta)\right)^{-1.5}, \quad (7)$$

where g is the asymmetry parameter, that is, the anisotropic of the fog (in our case $g = 0.7$) and θ is the scattering angle and is taken zero ($\theta = 0$) in the original beam light propagation.

Figure 6 shows the data obtained with the experimental setup to measure depolarization. These data were plotted and fitted with the Eq. (7).

3. Conclusions

In this work, we presented a novel way to measure the size of water droplets, of the fog to characterize. With the help of a microscope, model Titan TM-11, which has a minimum displacement of 0.0001 of inch (approx. two microns) we did a reference grid from a garlic cell; the distribution size was fitted fairly well with a generalized gamma function. With this gamma function we obtained the density droplets per unit volume. It was observed that the fog has different extinction coefficients at different wavelengths, there is a maximum difference between the wavelengths of 488 and 457 nm. At wavelengths of 476, 496, 514 and 632.8 nm the extinction coefficient does not changing so much. Finally, the depolarization plot shows that the forward lobule is very wide compared with the backward lobule, besides that the ratio is almost constant in the forward lobule.

Acknowledgements

This work has been sponsored by PROMEP, grant BUAP-EXB-718 and CONACYT 84008.

